A DEMODULATION SYSTEM FOR VECTOR MEASUREMENTS FROM

A SPINNING SATELLITE*

William J. Kerwin[†] and Robert Munõz[†]

A method has been developed for demodulating spin-modulated data from magnetometer sensors mounted on a spinning satellite. This system allows direct interpretation of data frequencies below, at, and above the spin frequency.

In simple data-gathering systems the process to be measured and the measuring instrument are normally contained in the same spatial frame of reference and the measurements made may be interpreted directly as a measure of the process. This is not the case when the measuring instrument is mounted on board a spinning platform. The input data to a vector magnetometer mounted on board a spinning satellite are modulated by the spinning. Some interpretation of this spin-modulated data is necessary before the original process can be clearly understood.

Since satellite spin frequencies lie within the band of frequencies of the data (normally in the order of 1 cps), it is necessary to demodulate the spin-modulated data in such a way that no errors are contributed by the demodulation technique. A technique has been developed which will allow accurate recovery of data measured on a spinning platform for frequencies below, at, and above the spin frequency.

Heretofore, amplitude demodulators such as the peak detector and the synchrodyne techniques have been used. But each of these is limited in its ability to pass frequencies equal to, or greater than, the modulation frequency which, in data gathered from a spinning platform, is the spin frequency. The simple peak detector consists of a rectifier and filter

combination in which the rectifier effectively samples the peak of each cycle of carrier and the filter fills in the gap between this cycle and the next. This type of circuit depends on a high degree of frequency separation between the maximum data frequency and the carrier frequency.

The synchrodyne technique shown functionally in Fig. 1 is also frequency limited. In this system, a reference signal identical in frequency to the carrier signal multiplies the modulated input to produce two sidebands at the sum and difference frequencies. The lower sideband of the modulated carrier extends from carrier frequency down to dc or zero frequency but may not extend beyond into the negative frequency regime if spectrum folding is to be avoided. If ideal filtering were possible, data could be recovered up to the carrier frequency, but no higher. This imposes a basic limitation on the input data. It must not have frequency content equal to or greater than the carrier frequency. The upper sideband is normally rejected and data are recovered from the lower sideband only.

The limitations imposed by the simple demodulators discussed above can be eliminated by the use of the two-phase demodulator shown in Fig. 2. Two directional sensors (vector component sensors in the spin plane) are mounted on a spinning platform with the axis of sensitivity of the first displaced by 90° from the axis of sensitivity of the second (to obtain the x and y components of the measured quantity). A two-phase oscillator is locked in both frequency and phase to the spinning platform by a sun pulse generator. These outputs are sin ωt, cos ωt. The output from each sensor is then multiplied by the two oscillator outputs as shown in Fig. 2 (four multipliers are required for this operation). After multiplication the signals are combined in summing amplifiers to produce a measure of the magnitude of the input information

resolved around a fixed coordinate system determined by the phase locked reference signal. The input information measured by the spinning sensors has thus been demodulated and separated into two orthogonal components. This method does not produce the errors normally encountered in peak demodulation, or in synchronous demodulation as discussed above.

Figure 3 shows the relative positions of the sensors and the positive direction of rotation ωt, as well as φ, the angle between the magnetic field and the reference direction.

Now we have as the output of sensor No. 1:

$$E_{S1} = H(t)\cos(\omega t - \varphi)$$

and as the output of sensor No. 2:

$$E_{S2} = H(t)\sin(\omega t - \varphi)$$

As shown in Fig. 2 we obtain, at the output of multiplier No. 1:

$$E_{S1} \sin \omega t = H(t)\cos(\omega t - \varphi)\sin \omega t$$

And at the output of multiplier No. 4:

$$E_{S2} \cos \omega t = H(t)\sin(\omega t - \varphi)\cos \omega t$$

These two terms are then subtracted in amplifier No. 1 (Fig. 2). This gives us:

$$\text{Output No. 1} = H(t)[\cos(\omega t - \varphi)\sin \omega t] - H(t)[\sin(\omega t - \varphi)\cos \omega t]$$

$$= \frac{H(t)}{2}[\sin(2\omega t - \varphi) + \sin \varphi] - \frac{H(t)}{2}[\sin(2\omega t - \varphi) - \sin \varphi]$$

$$= \underline{H(t)\sin \varphi}$$

By the same process, using multipliers 2 and 3, and adding their outputs, we have:

Output No. 2 = $H(t)[\cos(\omega t - \varphi)\cos \omega t] + H(t)[\sin(\omega t - \varphi)\sin \omega t]$

$$= \frac{H(t)}{2}[\cos(2\omega t - \varphi) + \cos \varphi] + \frac{H(t)}{2}[-\cos(2\omega t - \varphi) + \cos \varphi]$$

$$= \underline{H(t)\cos \varphi}$$

The two outputs, $\underline{H(t)\sin \varphi}$ and $\underline{H(t)\cos \varphi}$ are the two components of $H(t)$ projected in the reference direction and in a direction perpendicular to the reference direction. (See Fig. 3.) Both terms are independent of spin frequency. They measure the input data (in this case magnetic field $H(t)$) as though the sensors were mounted on a stationary platform with one sensor pointed in the reference direction, and the other perpendicular to that direction, and the two outputs allow for complete reconstruction of total amplitude and direction to as high a frequency as can be transmitted by the telemetry system.

A test of this demodulation system was made on an analog computer. Waveforms were recorded for various inputs corresponding to magnetic field variations at various simulated spin frequencies.

Figure 4 shows the output of the two-phase oscillator to identify the carrier frequency in succeeding figures. The time scale is the same on Figs. 4, 5, 6, and 7. Figure 5(a) shows the simulated input $H(t)$ at a frequency much below the carrier frequency; Figs. 5(b) and 5(c) show the modulated wave as would be produced by satellite spin at a frequency ω and an arbitrary phase angle φ on two sensors at right angles to each other; and Figs. 5(d) and 5(e) show the outputs of the demodulator

resolved into the two orthogonal components $H(t)\sin\varphi$ and $H(t)\cos\varphi$. The arbitrary scale factor is H (recording amplifier gain).

Similar waveforms are shown in Fig. 6, except that the input signal $H(t)$ is now equal to the carrier frequency. The drift in average value of the two waveforms of Figs. 6(b) and 6(c) is due to a slight phase slip between $H(t)$ and the reference signals.

Figure 7 shows the same waveform with the input signal of higher frequency than the carrier. The modulated waveforms of Figs. 7(b) and 7(c) would be very difficult to interpret without demodulation and, in addition, would be difficult to telemeter with sufficient accuracy to reconstruct the vector components, $H(t)\sin\varphi$ and $H(t)\cos\varphi$. Even though only sinusoidal variations of $H(t)$ are shown, any arbitrary waveform would be accurately demodulated by this technique. Steady-state values, square waves and the like are all possible. Vector readings of magnetic field may thus be made as though the spinning platform were standing still.

A slight variation of the demodulator system described above provides a carrier type communications system as shown in Fig. 8. This figure is much the same as Fig. 2, except that the two sensors on the spinning platform are replaced by a two-phase modulator. This diagram shows a data transmission system where the input process is modulated and transmitted over three channels and reproduced in a demodulator in such a way that frequency content can be transmitted below, at, and above the modulation frequencies. Data transmission Channel No. 1 in the diagram allows transmission of the in-phase part of the modulated data. Data transmission Channel No. 2 allows the transmission of the quadrature part of the modulated data while Channel No. 3 provides a phase-lock

between the modulating oscillator and the demodulating oscillator. In many systems, Channel No. 3 is not necessary because phase-lock can be obtained from either Channel No. 1 or Channel No. 2. The previous mathematical description of the system operation shown in Fig. 2 is an accurate description of the operation of this system. If there is no phase-shift between the modulating oscillator and the demodulating oscillator, the output of Channel No. 2 will be zero at all times and consequently all those elements shown in dashed lines may be removed from the system. Output No. 1 will then represent the complete magnitude of the input signal. This type of modulation process is useful in carrier systems where the carrier frequency must be in the band of frequencies ordinarily occupied by input information. Data amplifiers and tape recorders are two systems which could possibly benefit by the use of this modulating technique.

FOOTNOTES

*Received

†NASA, Ames Research Center, Moffett Field, California.
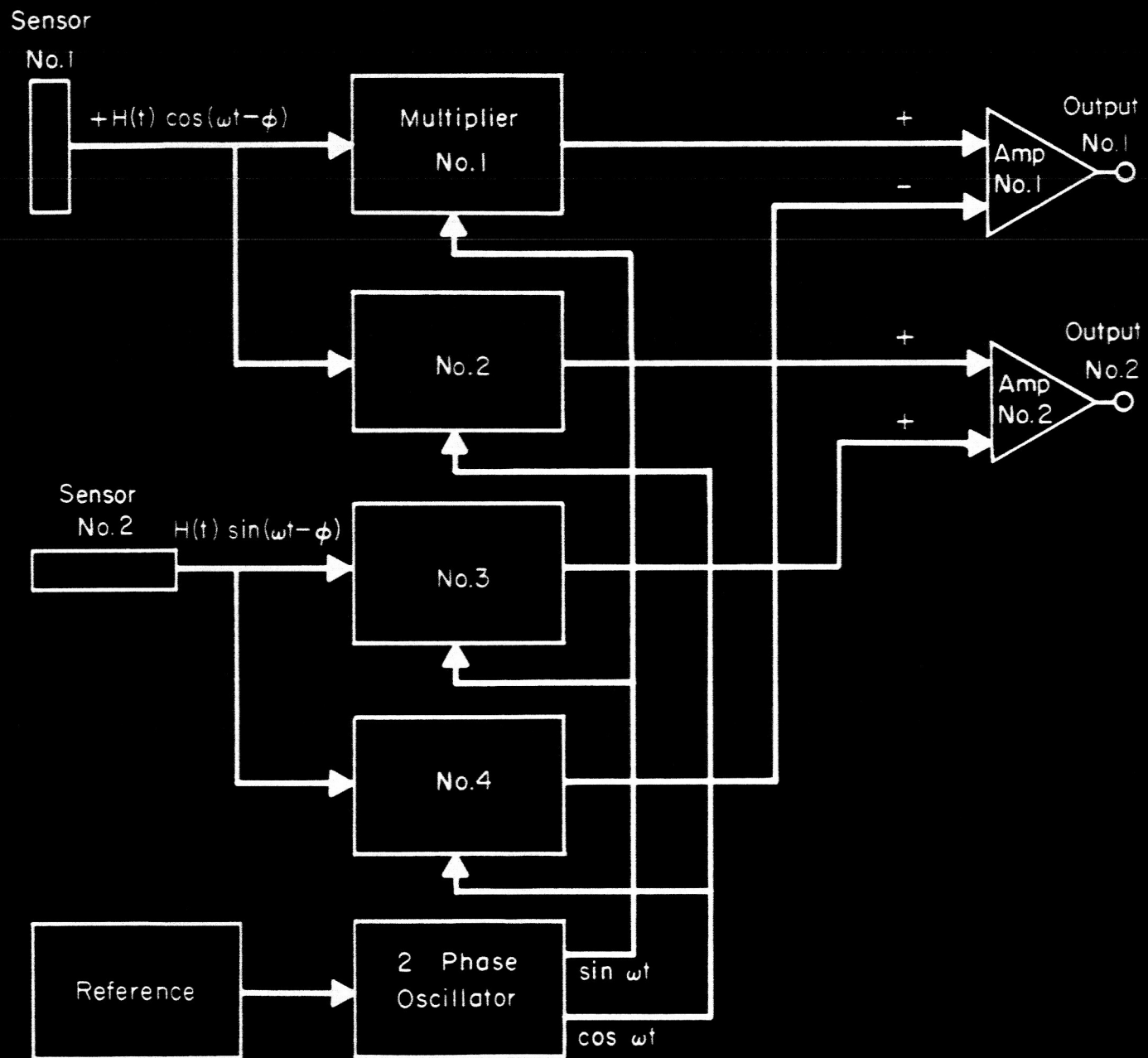
FIGURE LEGENDS

Fig. 1.- Two-phase demodulator.

Fig. 2.- Block diagram for two-phase demodulation system.

Fig. 3.- Sensor geometry.

Fig. 4.- Two-phase oscillator outputs.
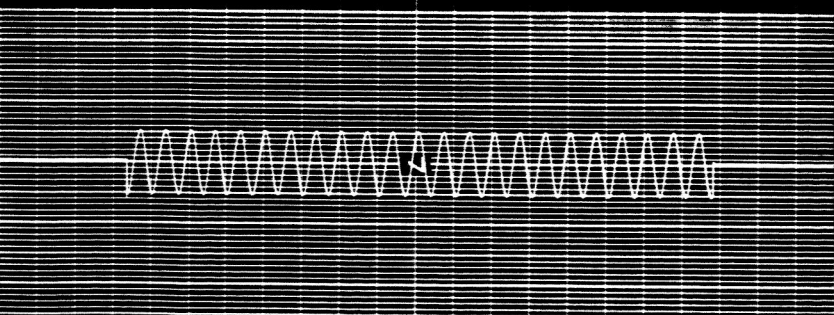
Fig. 5.- Demodulation waveforms for periodic input with frequency less than carrier frequency.

Fig. 6.- Demodulation waveforms for periodic input with frequency equal to carrier frequency.

Fig. 7.- Demodulation waveforms for periodic input with frequency greater than carrier frequency.

Fig. 8.- Two-phase modulation and demodulation system.
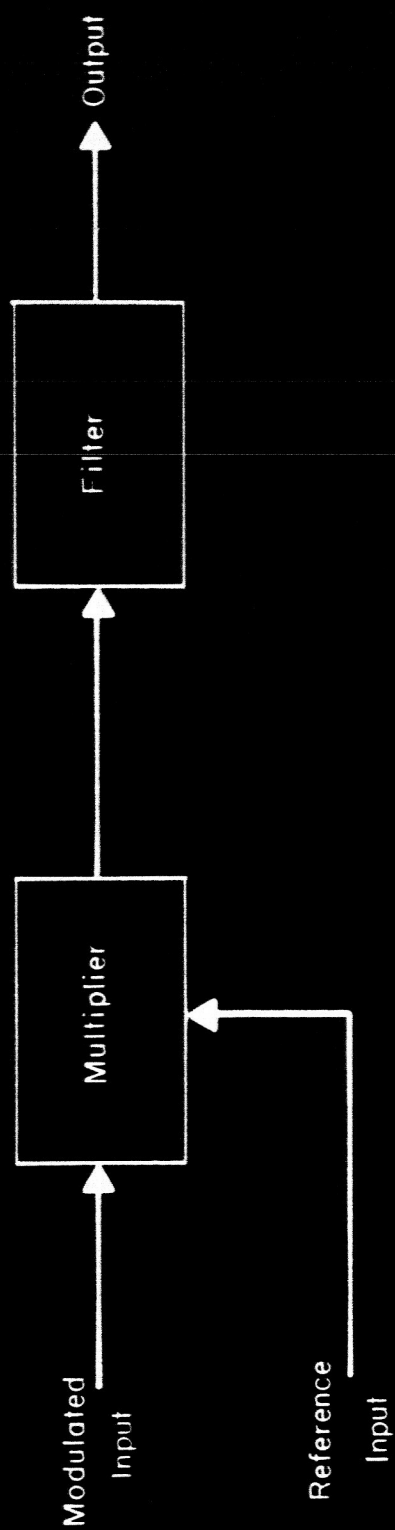
Fig. 1.– Synchrodyne demodulator.

Fig. 2.- Block diagram for two-phase demodulation system.

Fig. 3.— Sensor geometry.

(a) H(t)
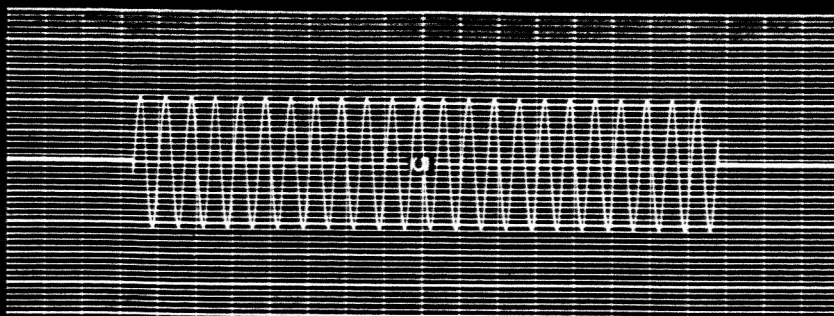
(b) H(t) sin(ωt - φ)
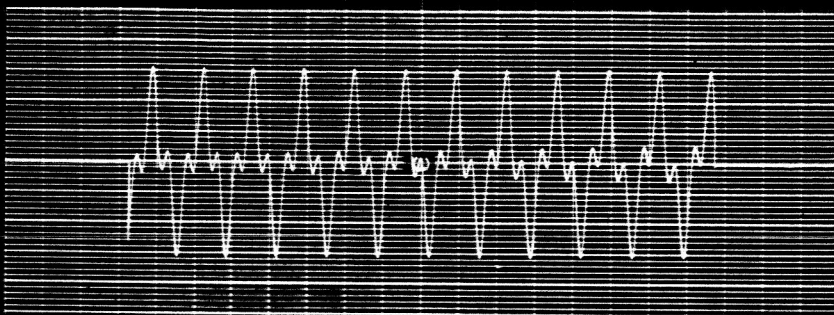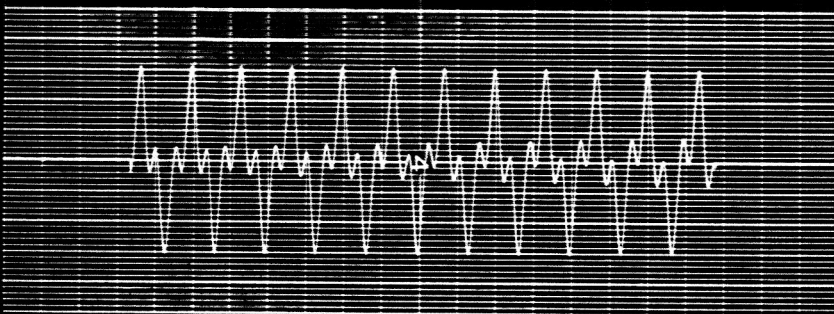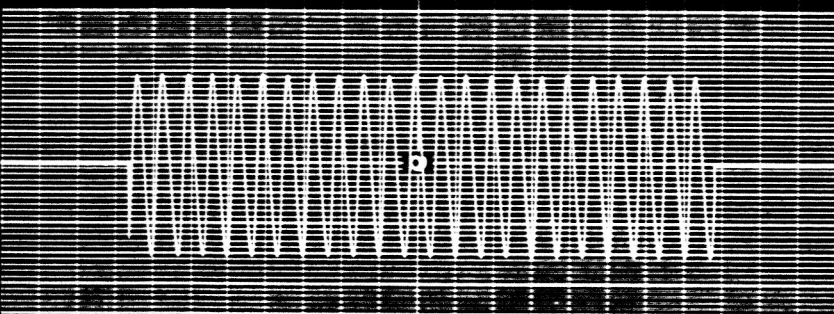
(c) H(t) cos(ωt - φ)

(d) KH(t) sin φ

(e) KH(t) cos φ

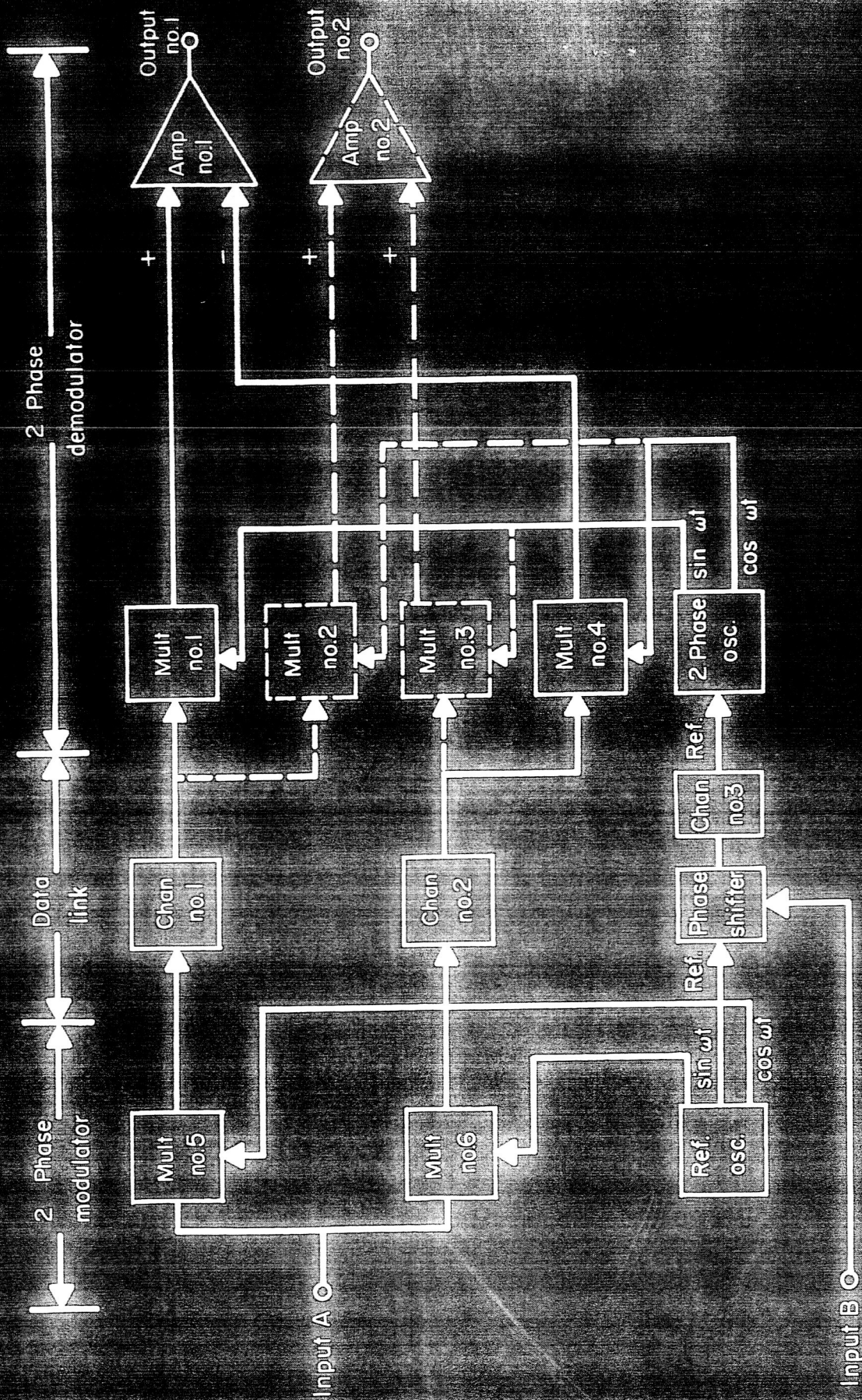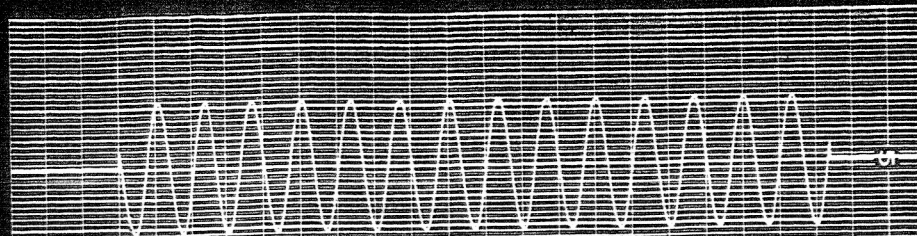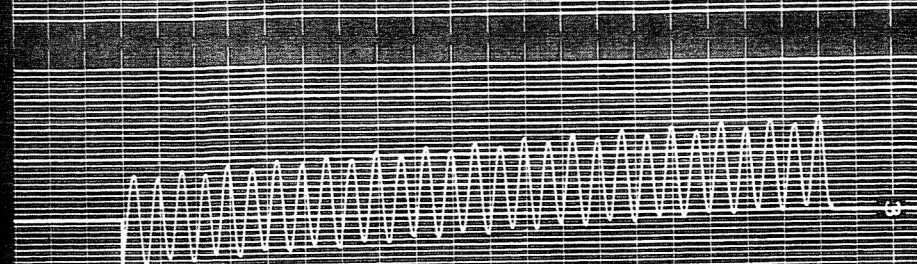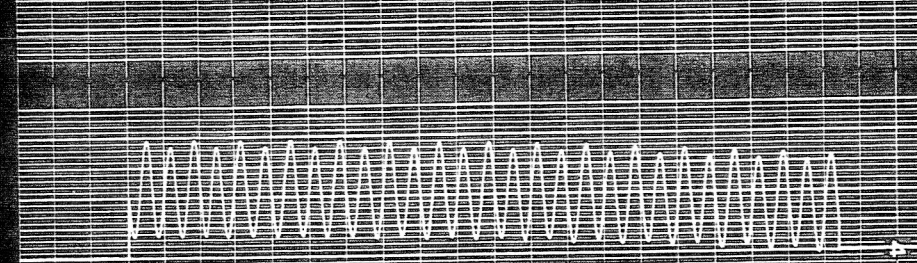Fig. 7.- Demodulation waveforms for periodic input with frequency greater than carrier frequency.

Fig. 8.— Two-phase modulation and demodulation system.

(a) $H(t)$
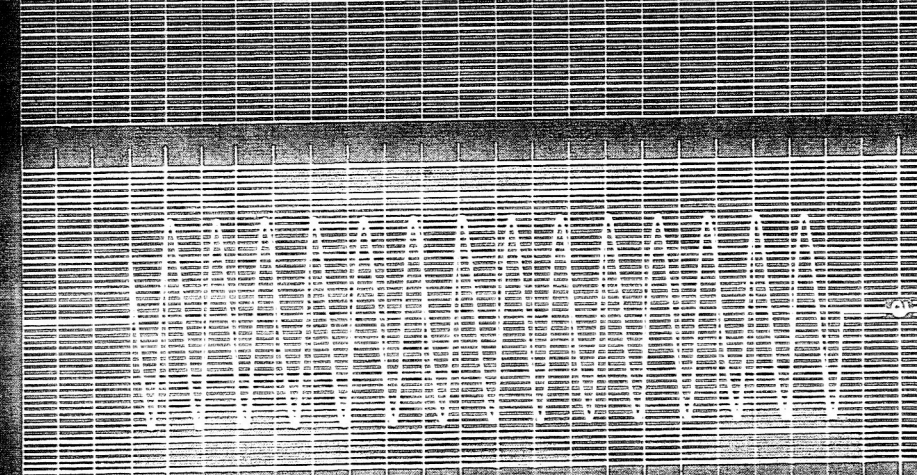
(b) $H(t)\sin(\omega t - \phi)$

(c) $H(t)\cos(\omega t - \phi)$
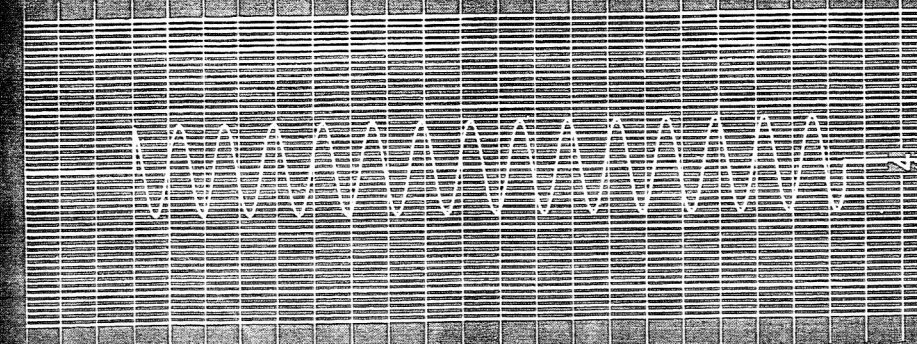
(d) $KH(t)\sin\phi$

(e) $KH(t)\cos\phi$

Fig. 6.- Demodulation waveforms for periodic input with frequency equal to carrier frequency.